

## Article

# Influence of Few-Layer Graphene on Frictional Properties of Lithium Compound Grease

Yanshuang Wang <sup>1,2,\*</sup>, Zizhen Liu <sup>1,2</sup>, Xudong Gao <sup>1,2</sup>, Qingguo Qiu <sup>1,2</sup> and Mingwei Wang <sup>1,2</sup>

<sup>1</sup> School of Mechanical Engineering, Qilu University of Technology (Shandong Academy of Sciences), Jinan 250353, China; zizhen\_liu99@163.com (Z.L.); gg824032455@163.com (X.G.); qqg991217@163.com (Q.Q.); mingwei\_wang\_wf@163.com (M.W.)

<sup>2</sup> Shandong Institute of Mechanical Design and Research, Jinan 250031, China

\* Correspondence: hkd\_wang\_yan\_shuang@126.com; Tel.: +86-182-2264-1850

**Abstract:** The frictional properties of lithium compound grease (LCG) with different percentage compositions of few-layer graphene (FLG) were investigated, and the mechanisms of temperature and loading effects on LCG containing FLG are also considered. The concluding effect shows that 1 wt% FLG is more appropriate for friction and wear modifiers for lithium compound grease at elevated temperatures and less suitable at ordinary temperatures. Thickener chemisorption film, FLG layering film, and tribo-reaction film consisting of FeO(OH), Fe<sub>2</sub>O<sub>3</sub>, Fe<sub>3</sub>O<sub>4</sub>, Li<sub>2</sub>O, and other oxides assist in the establishment of a lubricating boundary film on the friction interfaces lubricated with LCG containing FLG. The poor fluidity of lithium compound grease at low temperatures leads to poor dispersion of FLG, decreasing friction reduction capability. Under elevated temperature and low load condition, adding 1wt% FLG to LCG can only improve its wear-resistant property, the abrasion volume of steel plate reduced by 24.49%. Under elevated temperature and high load condition, adding 1wt% FLG to LCG can only enhance its anti-friction characteristics. Conversely, FLG is unsuitable as an anti-friction and wear-resistant additive for LCG at low-temperature conditions.

**Keywords:** few-layer graphene; lithium compound grease; frictional mechanism; abrasion scar; friction coefficient



**Citation:** Wang, Y.; Liu, Z.; Gao, X.; Qiu, Q.; Wang, M. Influence of Few-Layer Graphene on Frictional Properties of Lithium Compound Grease. *Coatings* **2024**, *14*, 561. <https://doi.org/10.3390/coatings14050561>

Academic Editor: Jose Luis Viesca

Received: 25 March 2024

Revised: 27 April 2024

Accepted: 30 April 2024

Published: 1 May 2024



**Copyright:** © 2024 by the authors. Licensee MDPI, Basel, Switzerland. This article is an open access article distributed under the terms and conditions of the Creative Commons Attribution (CC BY) license (<https://creativecommons.org/licenses/by/4.0/>).

## 1. Introduction

Many scholars have researched the impact of nano-additives, including but not limited to nano talc particles [1], PTFE particles, nano PTFE particles [2], nano CeO<sub>2</sub> [3], and nano CuO [4]. Wu Can et al. prepared LCG with various additives such as black carbon, nano Fe<sub>3</sub>O<sub>4</sub>, and nano Al<sub>2</sub>O<sub>3</sub>, and when the tribological properties of LCG with nano-additives were compared with pure LCG, they found that LCG with nano-additives had better tribological properties [5,6]. They also investigated the synergistic effects of hexagonal boron nitride and rigid shell flexible core nanocomposites (ZnO@SiO<sub>2</sub>) as well as various additives on the frictional properties of greases [7]. It has been demonstrated that these additives exhibit varying degrees of improvement in frictional performance. Among nano-additives, graphene has become a research hotspot in tribology due to its exceptional mechanical strength, ultra-thinness, atomic-level smooth surface, low interlayer shear, and robust chemical stability [8,9].

In recent years, numerous domestic and international scholars have incorporated graphene into various greases to investigate their friction characteristics [10]. The findings suggest that the inclusion of graphene augments the grease's capacity to bear loads, while also promoting the development of a boundary film and friction chemical interaction film on the worn surface, thereby enhancing both anti-friction and wear-resistant capabilities [11,12]. The facile exfoliation of graphene promotes the formation of the boundary films during friction, which not only hinders straight contact between the frictional counterparts and enhances the flexibility and self-adaptability of the frictional contact area but also

facilitates lubrication through lessening potential energy barriers between layers due to large interlayer gap in the boundary film and weak van der Waals forces among layers [13].

The greater the original content of graphene exfoliation and the more even its dispersion, the better the frictional properties [14,15]. The protective film formed by the graphene layer shearing on the sliding contact interface is strongly associated with the graphene structure and the surface texture of the friction substrate, indicating an integrated effect between the graphene additive and the surface deformation of the tribological substrate, not just the straightforward overlay of the two [16]. Lithium grease stands as one of the most frequently utilized greases. There have been numerous studies on the incorporation of graphene into lithium greases. It was discovered that the incorporation of graphene not only protected the rubbing surface but also promoted the generation of  $\text{Fe}_2\text{O}_3$  and  $\text{Li}_2\text{O}$  friction film, and the synergistic effect with deposited film and friction tribo-film obviously improved the frictional characteristics of lithium grease, improved the wear-resistant performance and friction reduction performance of the grease, and improved the sintering point and load wear index [15–19].

Graphene derivatives as grease additives have superior friction and wear properties, even better than conventional graphene additives. Graphene oxide, a common graphene derivative, also has excellent frictional properties as a grease additive [20,21]. In addition, graphene derivatives such as three-dimensional layered porous graphene, different forms of graphitic carbon nitrides, and fluorinated graphite have been prepared, all of which enhance the lubricating capacity, friction reduction, and wear-resistant capacity of greases [22–24]. Graphene compounds such as  $\text{Mn}_3\text{O}_4$ /graphene and  $\text{MoS}_2$ /reduced graphene oxide also have excellent frictional properties [25,26].

Graphene typically has a layer spacing of 3.55 Å. When the number of graphene layers is less than 10, it is called FLG. Li ZJ et al. incorporated few-layer graphene as an additive into lithium grease. They performed friction experiments using the MR-10P four-sphere friction tester and found that lithium grease added 0.1 wt% FLG had excellent friction reduction and abrasion resistance at higher loads and slower speeds. The primary constituent of its chemically reactive film formed on the worn surface of pure lithium grease is  $\text{Fe}_3\text{O}_4$ , while the boundary film of lithium grease containing FLG consists mainly of  $\text{Fe}_2\text{O}_3$  and adsorbed FLG [27]. Cheng ZL et al. prepared FLG using the  $\text{Li} + / \text{Na} +$  co-intercalation layer peeling method supported by the ultrasonic way, and the thickness of the exfoliated FLG was about 2.38–2.56 nm (about 7–8 layers). FLG was added to the grease, and friction testing was performed using a four-sphere friction testing machine. It was found that the grease with 0.06 wt% FLG added exhibited superior frictional wear-resistant performance, which improved by 21.35% and 30.32%, respectively, compared with unmixed grease [28].

Graphene, as a grease additive, is not suitable in all cases. Sun Z et al. added multilayered graphene and micron graphite to IRIS-200BB wire rope specialty grease. It was found that, for the protruding friction configuration of the four-ball machine, adding various additives effectively improved the characteristics of reduced friction and abrasion resistance of the basic grease. Still, when the micro-dynamic tribological behavior of the spiral-structured metallic filament subjected to varying lubrication scenarios was studied, the frictional characteristics of the graphene composite grease were instead inferior to the base grease for the concave friction form [29]. Mohamed A et al. integrated graphene and multi-layered carbon nanotubes as additives into a compound calcium grease in a 1:1 ratio. When the additive content exceeded 2 wt%, graphene began to break down and aggregate, reducing the frictional characteristics of the grease [30].

Whether graphene is appropriate for grease slip-enhancing and wear-reducing additives is also controversial and should depend on the type of grease, the working conditions, and the graphene content. Whether graphene is appropriate for a grease slip-enhancing and wear-reducing additive needs to be judged by tests.

To investigate the optimum content of FLG and the applicable working conditions of LCG with FLG added, LCG with different FLG contents were prepared in this study, and

the prepared LCG were subjected to friction tests at different temperatures and different load conditions using an SRV-5 rubbing and abrasion tester. Examination of the worn surface was done via XPS.

## 2. Materials and Methods

### 2.1. Test Materials

The FLG additive applied in this study is SE1231 graphene, produced by Changzhou Sixth Element Company. SE1231 type graphene is black powder in appearance with a mean particle size D50 below 10.0  $\mu\text{m}$ . The grease used in this test is LCG. The LCG utilizes PAO oil as its basic oil, exhibiting a viscosity measurement of 68 cst. The basic parameters of base oil are given in Table 1.

**Table 1.** The basic parameters of base oil at 30 °C.

Base Oil	Dynamic Viscosity $\eta$ (mPa·s)	Viscosity-Pressure Coefficient $\alpha$ ( $10^{-8} \text{ Pa}^{-1}$ )
PAO	$92.12 \pm 0.09$	1.7

The thickener material was dodecahydroxystearic acid with a content of 15%, as shown in Figure 1. The saponification reaction was facilitated by the addition of a lithium hydroxide aqueous solution. Then stearic acid was added as a compound agent for the compound reaction to generate the LCG, whose thickening structure is shown in Figure 1. Lithium compound greases with different FLG contents were configured with 0, 0.5 wt%, 1 wt%, and 2 wt%, respectively. The FLG in the LCG is fully dispersed using the physical dispersion method.

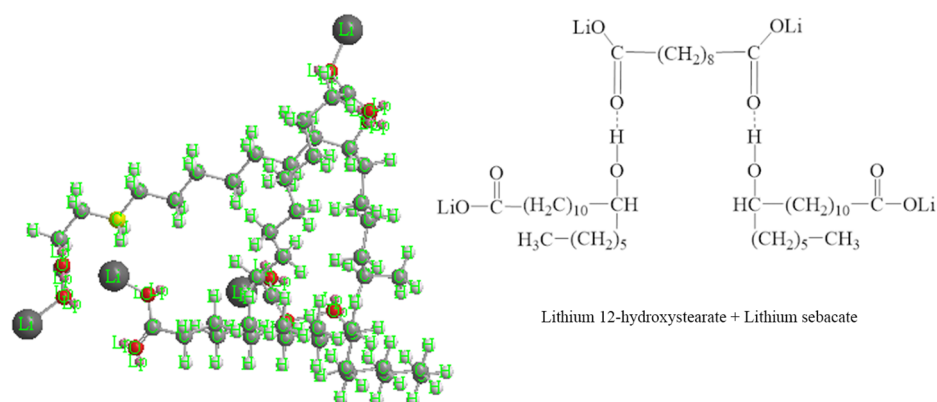


**Figure 1.** Chemical configuration of thickener for lithium compound grease.

### 2.2. Experimental Procedure

The frictional characteristic of the grease samples was tested using the SRV-5 frictional abrasion test machine (Figure 2). The above friction interface comprises a GCr15 bearing steel ball, measuring 10.2 mm in diameter with a hardness of 59–61 HRC and a grade accuracy of G10 [31]. The GCr15 bearing steel plate, with a diameter of 24 mm, constitutes the lower friction interface. The test was performed in a reciprocal vibration mode with the test parameters given in Table 2. The maximum contact stresses during friction are 1 GPa and 2.06 GPa, respectively. To minimize testing inaccuracies, the friction experiment is replicated three times for each operational condition. The friction coefficient values of repeated tests are very close, and the rules of friction curves are highly consistent and have high repeatability. The two-dimensional and three-dimensional morphology of the steel plate surface corresponding to the friction curve was characterized. The average value of the abrasion volume after three tests is taken as the result of wear resistant performance, and shown in the following figures. The MIT300 metallurgical microscope was used to

observe the abrasion scars on the plate surface and to obtain the surface morphology of the abrasion scars on the plate. A Contour Elite K 3D optical profiler based on the principle of non-contact white-light scanning interferometry was used to obtain 3D morphological and sectional views of the abrasion scars on the plate surfaces and to measure the volume of abrasion scars. The length of the scanning area was set to a fixed value of 720  $\mu\text{m}$ , and the scanning width was adjusted according to the width of the steel plate abrasion scars, which was larger than the width of the abrasion scars, to obtain an accurate abrasion volume.

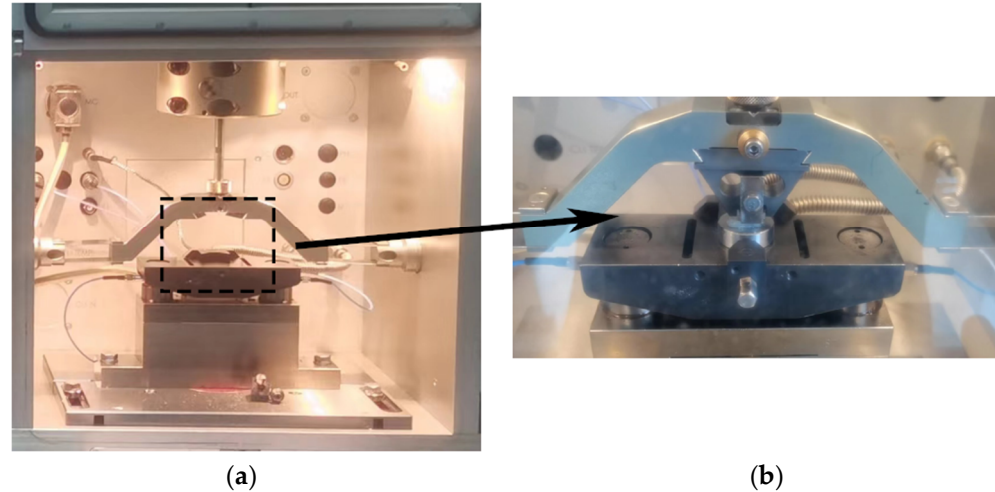


**Figure 2.** Wear testing equipment and sketch diagram of tribology principle: (a) SRV-5; (b) Test platform.

**Table 2.** Frictional experimental parameters.

Test Parameters	Load (N)	Temperature (°C)	Time (s)	Frequency (Hz)	Amplitude (mm)
Test conditions	10	30,100	1800	10	4
	90	30,100	1800	10	4

The elemental composition and chemical state of the surface of the steel plate were analyzed using an ESCALABXi + X-ray photoelectron spectrometer with a scanning depth of 1.5 nm. The XPS spectra of the worn surface were divided into peaks using the XPS peak4.1 software. And the chemical valence states of the elements on the worn surface were obtained by determining the binding energies of each peak from the binding energies of the different elements represented in the standard comparison card.

It is necessary to find out the status of lubrication between the ball and plate under this test condition, which will become the basis for establishing the friction mechanism model in the later stage. Before the experiment, the film thickness ratio  $\lambda$  is obtained by calculating the ratio of the minimum oil film thickness to the surface roughness of the friction pair, as shown in Equation (1):

$$\lambda = h_{min} / \sqrt{\sigma_1^2 + \sigma_2^2}, \quad (1)$$

In Equation (1):  $h_{min}$  is the minimum oil film thickness of the grease ( $\mu\text{m}$ ),  $\sigma_1$  and  $\sigma_2$  are the roughness Rq of the surfaces of the two friction pairs. The minimum oil film thickness under point contact can be estimated by the Hamrock–Dowson formula [32]:

$$h_{min} = 3.63U^{*0.68}G^{*0.49}W^{*-0.073}(1 - e^{-0.68k})R, \quad (2)$$

In Equation (2):  $U^*$  ( $=\eta U/E^*R$ ) is the dimensionless speed parameter,  $G^*$  ( $=\alpha E^*$ ) is the dimensionless material parameter,  $W^*$  ( $=W/(E^*R^2)$ ) is the dimensionless load parameter,  $k$

is the ellipticity,  $E^*$  is the equivalent elastic shear modulus, and  $R$  is the equivalent radius of curvature.

The tribological properties of LCG with different contents of FLG were measured by the SRV-5 frictional abrasion test machine. Depending on frequency and amplitude, its equivalent velocity  $U$  is 0.04 m/s. The contact load  $W$  between the ball and the disc is 10 N and 90 N. The surface roughness  $R_q$  of the ball and plate measured by the 3D white-light interference profilometer was about 0.125  $\mu\text{m}$  and 0.68  $\mu\text{m}$ , respectively. The film thickness ratios under low load and high load were 0.38 and 0.33, respectively. It is generally believed that  $\lambda < 1$ , the lubrication status is boundary lubrication.

### 2.3. Characterization of LCG Containing FLG before the Experiment

Figure 3 presents the infrared spectral analysis of four lithium compound greases. The base oil and thickener molecules of LCG contain a large number of alkanes; the absorption bands at 2840–2970  $\text{cm}^{-1}$  match with the tensile oscillation of  $-\text{CH}_3$  and  $-\text{CH}_2$ , and the absorption regions at 1380 and 1460  $\text{cm}^{-1}$  match the bending oscillation of  $-\text{CH}_3$  and  $-\text{CH}_2$ . The absorption peak at 720  $\text{cm}^{-1}$  matches the out-of-plane oscillation of  $(\text{CH}_2)_n$ . The absorbance peak at 1580  $\text{cm}^{-1}$  matches the stretching oscillation of the  $\text{C}=\text{O}$  group in the thickener molecule. Because the FLG does not contain functional groups, it has little impact on the infrared spectrum detection results of LCG and only reduces the absorbance because of its opacity.

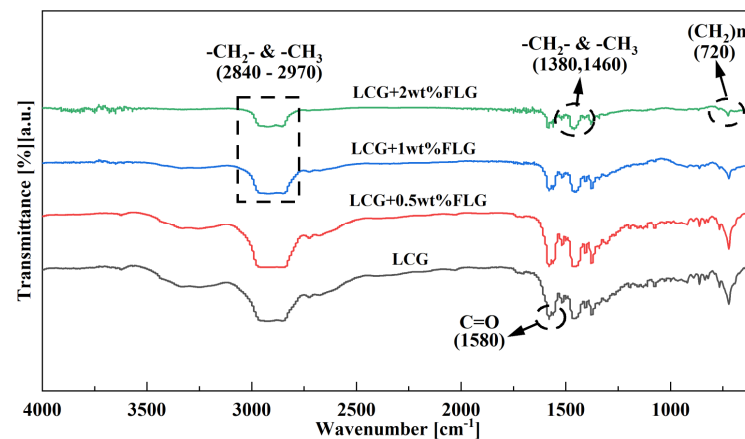


Figure 3. Fourier infrared spectra of four kinds of lithium compound greases.

Figure 4 exhibits the SEM imagery of thickener with pure LCG and LCG with 1 wt% FLG. As depicted in Figure 4, the microstructure of its thickener exhibits a highly intertwined fibrous structure, and the incorporation of FLG makes the fibrous structure closely adsorbed together with it.

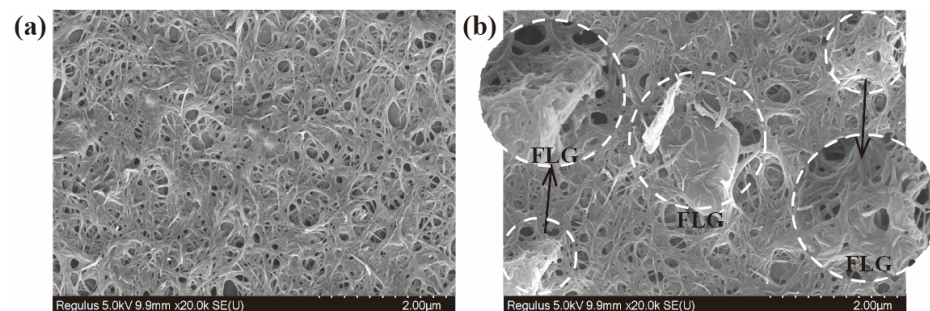


Figure 4. SEM images: (a) pure LCG; (b) LCG with 1 wt% FLG.

### 3. Results and Discussion

#### 3.1. Frictional Characteristics of Lithium Compound Grease

##### 3.1.1. Low Load and Low-Temperature Working Condition

Figure 5 shows the COF curves, the abrasion volume of the steel plate (SPAV), and two-dimension, three-dimensional, and sectional views of abrasion scars on the plate surfaces lubricated by LCG, LCG + 0.5 wt% FLG, LCG + 1 wt% FLG, and LCG + 2 wt% FLG, respectively, at a 10 N and 30 °C condition.

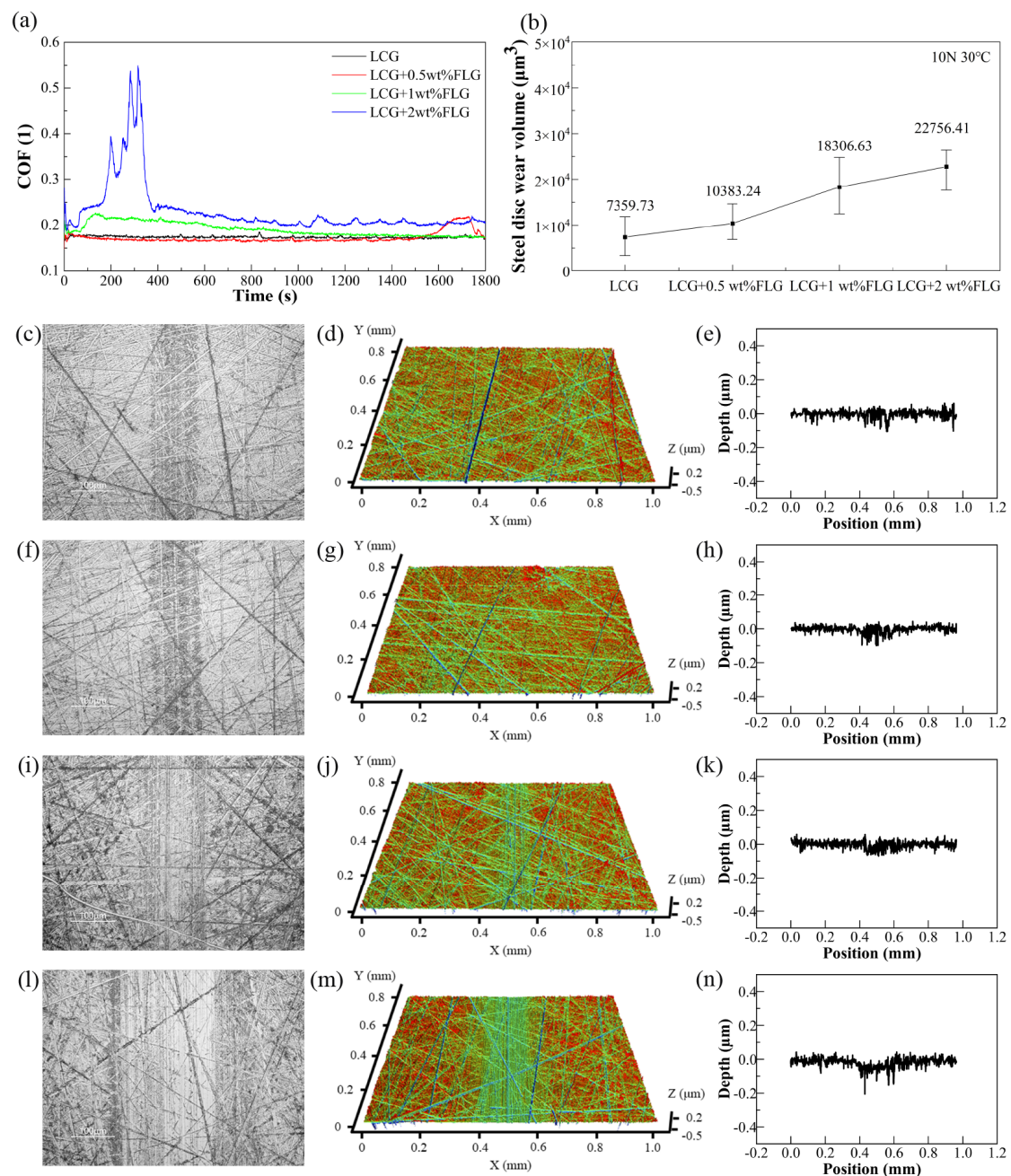


**Figure 5.** (a) COF curves of LCG; (b) abrasion volume of worn surfaces; (c,f,i,l) surface appearance of steel plate abrasion scars; (d,g,j,m) three-dimensional appearance of steel plate abrasion scars and; (e,h,k,n) sectional view of steel plate abrasion scars under 10 N, 30 °C.

Figure 5a shows the friction coefficient (COF) curves under the lubrication with four lithium compound greases at 10 N and 30 °C. The 0–30 s period is the initial break-in stage

of the friction process, the metal surface of the friction pairs have just started to contact, and the bumps on the friction surface crash into each other, resulting in a huge increase in the COF. In the running-in process, the lubricating film composed of LCG is progressively formed and the COF is gradually stable. At low load and low-temperature conditions, the COF curve for pure LCG is relatively stable with minor fluctuations, indicating that the lubricating film is relatively stable. Within 1500 s, the COF curve for LCG + 0.5 wt% FLG is highly stable and the COF is smaller than that of pure LCG. However, at 1500 s, the stable lubrication state is broken and the COF curve for LCG + 0.5 wt% FLG suddenly increases. Until 1800 s, the COF curve for LCG + 0.5 wt% FLG returns to a stable state. The COF curve for LCG + 1 wt% FLG gradually increases at 0–150 s and then decreases. Compared with pure LCG, LCG + 0.5 wt% FLG, and LCG + 1 wt% FLG, the LCG + 2 wt% FLG has a higher COF and a more fluctuating COF curve, and a sudden evolution occurred between 200–400 s. This is because with the higher content of FLG in LCG, the polymerization of FLG due to the van der Waals force is more serious, which results in large fluctuations in the friction curve. The stability of graphene depends on two forces: one is the bonded interaction between the carbon-carbon atoms and the other is the non-bonded interaction, that is the van der Waals force between layers, through which graphene piles up against each other [33]. The van der Waals force is related to the distance between the layers. When the distance is larger, the van der Waals force is smaller and it is easier to break through the energy barrier [13]. As the spacing decreases, the van der Waals force increases gradually. When the spacing reaches 0.425 nm, the van der Waals force reaches the maximum, and the graphene layers attract each other. At this time, continuing to reduce the spacing, the van der Waals force will gradually decrease; when the spacing reaches 0.3816 nm, the van der Waals force is zero, and the graphene polymer reaches stability [33]. The intensity of FLG in LCG + 2 wt% was the highest, and the polymerization phenomenon of FLG was the most serious, resulting in large fluctuations in the coefficient of friction within 200–400 s. The FLG could be rearranged by mechanical stripping of friction pairs [34]. Therefore, after 200–400 s of mechanical shear of friction pairs, FLG polymers were stripped and rearranged, a stable lubricating film was formed, and the COF tended to be stable. In addition, it can also be found from Figure 5m,n that there is a small amount of abrasive wear on the surface of the steel disc, which is caused by the FLG polymers acting as abrasive particles during the friction process. According to the above, FLG is disordered in LCG. During the early phase of friction, the COF fluctuates greatly. LCG with higher FLG content fluctuates more violently, which can also prove that FLG is disordered. After a period of friction, FLG gradually changed from randomness to arrangement, a stable lubricating film was formed, and the COF also tended to be stable.

Under low load and low-temperature conditions, the incorporation of FLG into LCG did not produce a positive influence on the anti-friction performance of LCG. When the COF tends to be stable, although the friction coefficient of LCG + 0.5 wt% FLG is lower than that of pure LCG, the lubrication process is susceptible to unstable factors, resulting in graphene disorder and causing fluctuations in the COF curve. The high FLG content of LCG will cause its COF to increase significantly, resulting in FLG requiring more time to transition from disorder to order, thereby necessitating additional time to form a stable lubricating film. Therefore, under low load and low-temperature condition, adding FLG to LCG will reduce its anti-friction performance.

Figure 5b shows the abrasion volume of the steel plate (SPAV) lubricated by four lithium compound greases. As shown in the figure, the SPAV of pure LCG is the smallest, and the higher the FLG content of LCG, the greater the SPAV. At low temperatures and low load conditions, FLG is easy to aggregate, and the polymerized FLG increases the SPAV, thereby reducing the wear-resistant performance of LCG.

Figure 5c–n shows the effects of LCG with different FLG contents. During lubrication with pure LCG and LCG + 0.5 wt% FLG, the abrasion scars on the steel plates are shallow, and the abrasion scars on the plate surfaces are brown and granular (Figure 5c,f) with

no obvious furrow formation, indicating that the friction pair is not in direct contact (Figure 5d,g). The wear type was oxidized wear and there was no abrasive wear.

Both sides of the abrasion scars on the plate surface lubricated with LCG + 1 wt% FLG show dark graininess, which is indicative of oxidative wear (Figure 5i). However, small furrows appeared in the middle of the abrasion scars on the plate surface, which is a manifestation of abrasive wear (Figure 5k). This phenomenon shows the polymerization of FLG appeared in LCG + 1 wt% FLG, and the polymerized FLG acted as abrasive particles, causing abrasive wear on the steel plate. Under the lubrication of LCG + 2 wt% FLG, the steel plates have the widest abrasion scars and more visible furrows (Figure 5l,m). The polymerization of FLG in LCG + 2 wt% FLG is higher, resulting in more serious wear on the steel plate, with significant depressions on the worn surface. Under low load and low-temperature conditions, the higher the content of FLG in LCG, the more obvious the furrows on the steel plate, because the higher the FLG content, the denser the distribution of FLG in the LCG. Under the action of the van der Waals force [33], FLG is prone to the polymerization phenomenon, forming larger graphene polymers. Graphene polymers act as abrasive particles during the friction process, causing abrasive wear and resulting in furrows on the plate surface. This phenomenon also shows that the lubricating film formed by pure LCG is more stable and can protect the friction surface under low load and low-temperature working conditions. Meanwhile, the polymerization of FLG is the main factor of furrow formation.

### 3.1.2. Low Load and High-Temperature Working Condition

Figure 6 shows the COF curves and the abrasion volume of the steel plate (SPAV) and two-dimension, three-dimensional, and sectional views of abrasion scars on the plate surfaces lubricated by LCG, LCG + 0.5 wt% FLG, LCG + 1 wt% FLG, and LCG + 2 wt% FLG, respectively, at a 10 N and 100 °C condition.

Figure 6a shows the COF curves under the lubrication with four lithium compound greases at 10 N and 100 °C. Under this working condition, after the initial run-in stage of 30 s, the COF of pure LCG is gradually reduced, a stable lubricating film is progressively formed after 200 s, and the friction coefficient is very smooth and basically maintained at about 0.18. The COF of LCG + 0.5 wt% FLG and LCG + 2 wt% FLG did not continue to decline after 30 s but stabilized at about 0.2. After an initial run-in period of 30 s, the COF of LCG + 1 wt% FLG plummeted to 0.18.

After FLG was added, the COF curve of LCG showed fluctuation and undulation, indicating that the lubricating film was unstable. The COF curve for pure LCG was very smooth and showed no fluctuations. This indicates that FLG, as an additive of LCG, makes it difficult to maintain an orderly state during friction at low load and high-temperature conditions. The disorder polymerization of FLG will lead to the instability of the COF in the lubrication process, so FLG has no obvious improvement on the anti-friction performance of LCG under a low load and high temperature.

Figure 6b shows the SPAV line chart of four kinds of lithium compound greases under low load and high-temperature conditions. In the figure, the disc lubricated with LCG + 1 wt% FLG has the smallest SPAV, reduced by 24.49%. LCG + 0.5 wt% FLG and LCG + 2 wt% FLG have larger SPAV than that of pure LCG. These results indicate that too much or too little FLG can increase the SPAV, and enhancing the wear-resistant performance of LCG is solely achievable with the exact content of FLG.

Figure 6c–n shows the effects of LCG with different FLG contents, respectively. Under the lubrication of the four lithium compound greases, the abrasion scars on the plate surfaces are shallow and appear dark granular wear (Figure 6c,f,i,l), and no obvious furrows are formed (Figure 6e,h,k,n), indicating that there is no direct contact between the friction pairs. The wear type is oxidative wear and there is no abrasive wear. The depth of the abrasion scars is not more than 0.1 μm. The plate surfaces lubricated by pure LCG and LCG + 1 wt% FLG have the shallowest abrasion scars (Figure 6e,k), and the cross-sectional views show that only a small number of burrs appear in the abrasion scars on plate surfaces.

With the lubrication of LCG + 0.5 wt% FLG and LCG + 2 wt% FLG, the abrasion scars on the plate surface showed a slight depression (Figure 6h,n). Among the samples, the steel plate lubricated with LCG + 0.5 wt% FLG has the widest surface abrasion scars (Figure 6f). Steel plates lubricated by LCG + 2 wt% LCG have narrow surface abrasion scars (Figure 6l,n), but the wear is more concentrated.

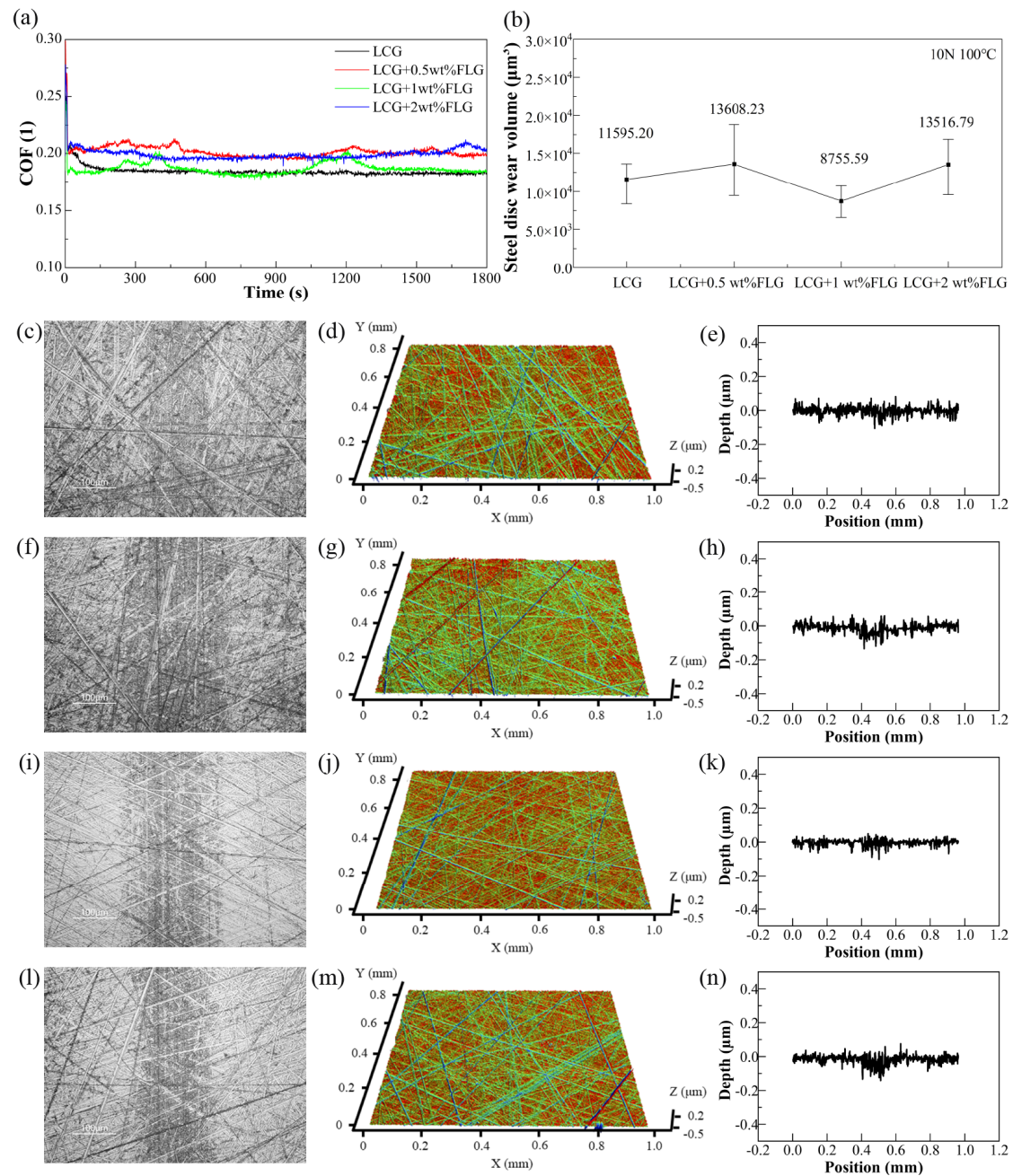


**Figure 6.** (a) COF curves of LCG; (b) abrasion volume of worn surfaces; (c,f,i,l) surface appearance of steel plate abrasion scars; (d,g,j,m) three-dimensional appearance of steel plate abrasion scars and; (e,h,k,n) sectional view of steel plate abrasion scars under 10 N, 100 °C.

Under low load and high-temperature conditions, the abrasion scars on the plate surfaces lubricated with four lithium compound greases are shallow, and the wear type is oxidative wear. An appropriate amount of FLG (1 wt%) can protect the friction surface, reduce abrasion, and improve the wear-resistant performance of LCG. Too little or too much FLG will increase abrasion.

### 3.1.3. High Load and Low-Temperature Working Condition

Figure 7 shows the COF curves and the abrasion volume of the steel plate (SPAV) and two-dimension, three-dimensional, and sectional views of abrasion scars on the plate surfaces lubricated by LCG, LCG + 0.5 wt% FLG, LCG + 1 wt% FLG, and LCG + 2 wt% FLG, respectively, at a 90 N and 30 °C condition.

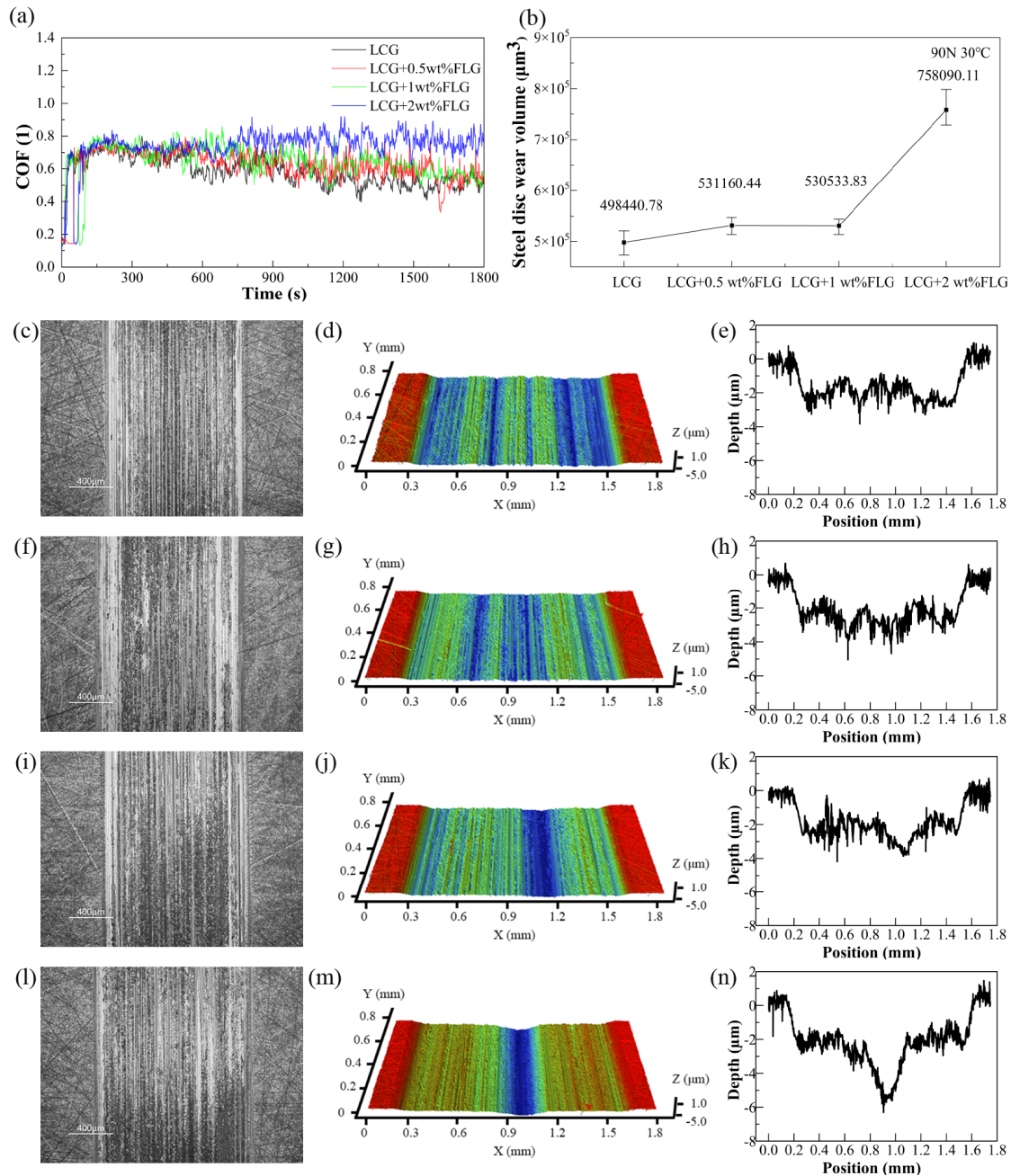


**Figure 7.** (a) COF curves of LCG; (b) abrasion volume of worn surfaces; (c,f,i,l) surface appearance of steel plate abrasion scars; (d,g,j,m) three-dimensional appearance of steel plate abrasion scars and; (e,h,k,n) sectional view of steel plate abrasion scars under 90 N, 30 °C.

Figure 7a shows the COF curves under the lubrication with four lithium compound greases. Under high load and low-temperature conditions, the friction coefficients rise rapidly to 0.7 within 100 s, which is much higher than that of the other three working conditions. The COF curve for pure LCG shows a downward trend in violent fluctuations. In the fluctuation process, every increase in the COF curve represents the destruction

of the lubricating film, and the grease enters the furrows on the worn surface again to supplement the lubricating film, resulting in a short decline in the COF. The fluctuation curves of four lithium compound greases indicate that the LCG is not suitable for high load and low-temperature conditions, and the lubricating film is unstable, resulting in poor anti-friction performance. In addition, FLG is easy to aggregate due to the increased load, which also reduces the anti-friction performance of LCG.

Figure 7b shows the SPAV line chart of four kinds of lithium compound greases under low load and high-temperature conditions. Similar to anti-friction performance, the SPAV of the four greases under low load and high-temperature conditions is much greater than that of the other three working conditions. The incorporation of FLG will increase the SPAV, indicating that FLG polymerization will also reduce the wear-resistant performance of LCG under high load and low-temperature conditions.

Figure 7c–n shows the effects of LCG with different FLG contents, respectively. Obviously, the width of the abrasion scars on the plate surfaces lubricated by four greases is far more than that of the other conditions. The dense furrows in the abrasion scars are caused by abrasive wear. The furrows of pure LCG are evenly distributed, and the depth of the abrasion scars is mostly 2–3  $\mu\text{m}$ . The most serious wear is mainly distributed on the edge of both sides, and the deepest abrasion scars reach 4  $\mu\text{m}$  (Figure 7d,e). The steel plate surface lubricated by LCG + 0.5 wt% FLG is also severely worn. The cross-sectional views show that the effect on both sides of the abrasion scars is roughly the same as that of pure LCG, but the wear in the middle position is significantly more serious (Figure 7g). Under the lubrication of LCG + 1 wt% FLG, the middle of the steel plate has more serious wear, the furrows of abrasion scars are more concentrated, and the wear depth reaches its maximum in the middle position (Figure 7j). This also suggests that the concentration of abrasive furrows is due to the production of FLG polymerization. Under the lubrication of LCG + 2 wt% FLG, the abrasion scars on the plate surface are the widest, and the wear in the middle of the steel plate is the most serious, the maximum depth of the abrasion is 6  $\mu\text{m}$  (Figure 7n).

It can be concluded that under high load and low-temperature conditions, the FLG is easy to aggregate, causing stress concentration and wear concentration in the middle of the plate, forming deeper furrows, and reducing the anti-friction and the wear-resistant performance of LCG.

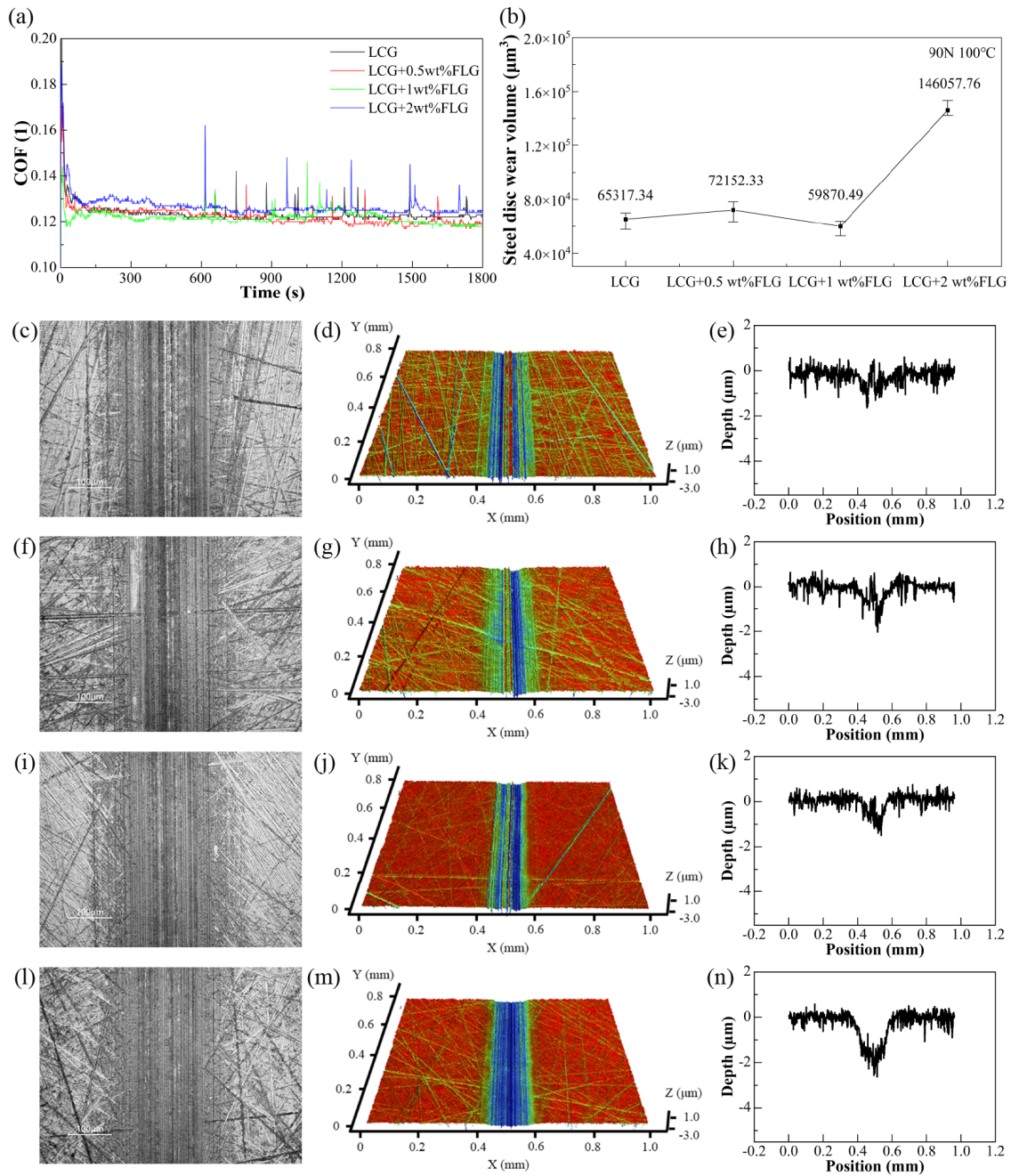
#### 3.1.4. High Load and High-Temperature Working Condition

Figure 8 shows the COF curves and the abrasion volume of the steel plate (SPAV) and two-dimension, three-dimensional, and sectional views of abrasion scars on the plate surfaces lubricated by LCG, LCG + 0.5 wt% FLG, LCG + 1 wt% FLG, and LCG + 2 wt% FLG, respectively, at a 90 N and 100 °C condition.

Figure 8a shows the COF curves under the lubrication with four lithium compound greases at 90 N and 100 °C. Under the condition of elevated load and high temperature, within 0–150 s of the initial run-in process, the COF of LCG with four FLG contents gradually decreases, and then the COF is relatively stable. However, after 600 s, the friction pair appeared stuck and sintered, and the COF began to increase instantaneously. Under high load and high-temperature conditions, LCG + 0.5 wt% FLG and LCG + 1 wt% FLG have lower friction coefficients than that of pure LCG, while LCG + 2 wt% FLG has higher COF than that of pure LCG. This phenomenon shows that the anti-friction performance of LCG can be improved with appropriate FLG under high load and high-temperature conditions. On the contrary, excess FLG will aggregate, resulting in increased COF.

Figure 8b shows the SPAV line chart of four kinds of lithium compound greases under high load and high-temperature conditions. Under this condition, compared with pure LCG, only LCG + 1 wt% FLG has slightly better wear resistance performance than pure LCG, and its corresponding SPAV is reduced by 8.34%. It can even be considered within the error scatter range, but too little or too much FLG will increase the wear rate. Under the lubrication of four greases, the SPAV of LCG + 0.5 wt% FLG and LCG + 2 wt% FLG was

greater than that of pure LCG, with an increase of 10.46% and 123.61%, respectively. This shows that under high load and high-temperature conditions, the addition of FLG has no significant effect on the wear resistance of LCG.



**Figure 8.** (a) COF curves of LCG; (b) abrasion volume of worn surfaces; (c,f,i,l) surface appearance of steel plate abrasion scars; (d,g,j,m) three-dimensional appearance of steel plate abrasion scars and; (e,h,k,n) sectional view of steel plate abrasion scars under 90 N, 100 °C.

Figure 8c–n shows the effects of LCG with different FLG contents. It can be seen that, under this condition, the abrasion scars on the steel plate surface of both sides are brown and granular and there are obvious furrows in the middle position, which indicates that the wear types of abrasion scars on the plate surfaces are abrasive wear and oxidative wear. The abrasion scars on the plate surface with the lubrication of pure LCG have obvious furrows, and the center of the abrasion scars is relatively intact, with two deep furrows on

either side of the worn center (Figure 8d). The left furrow had more severe wear, with a depth of about 1.5  $\mu\text{m}$  (Figure 8e). The shape of abrasion scars on plate surfaces lubricated by LCG + 0.5 wt% FLG and pure LCG are similar. The center of abrasion scars on the plate surface are also more complete, and the right furrow is the deepest, with a depth of 2  $\mu\text{m}$  (Figure 8h). The abrasion scars on the plate surface lubricated by LCG + 1 wt% FLG are also divided into two parts, but their depth is the shallowest. The deepest position of the scar is about 1  $\mu\text{m}$  (Figure 8k). The abrasion scar on the plate surface lubricated with LCG + 2 wt% FLG has a different shape from the other three greases, the middle position of the abrasion scar is not complete, and the entire abrasion scar is concave into the plate surface. The depth of the scar is the deepest and the wear is the most severe. The overall depth of the scar is about 2  $\mu\text{m}$  (Figure 8n).

Under the condition of high load and high temperature, the wear types of scars on plate surfaces lubricated with four lithium greases are abrasive wear and oxidative wear. With the increase of FLG content, the shape of the abrasion scars on plate surfaces gradually changed from intensive furrow to concentrated wear. This phenomenon indicates that the polymerization caused by excess FLG can concentrate the stress on the friction surface, leading to more severe abrasive wear.

### 3.2. Comparative Analysis of FLG with Other Nano-Additives

After frictional performance testing under four different operating conditions, we found that, under high-temperature conditions, only 1 wt% of FLG showed varying degrees of enhancement in the wear-resistant capability of LCG. In particular, under high-temperature and low load conditions, the SPAV lubricated with LCG + 1 wt% FLG decreased by 24.49% compared to pure LCG, demonstrating fine wear-resistant capability, although its anti-friction performance was inferior to that of pure LCG. However, under high-temperature and high load conditions, the SPAV lubricated with LCG + 1 wt% FLG decreased by 8.34%, only slightly improving the wear-resistant capability of LCG. This value could even be considered within the range of error scatter range. However, the friction coefficient is lower than that of pure LCG, indicating a slight improvement in friction reduction capability. However, adding FLG to LCG under low-temperature conditions can have a negative impact on the tribological performance of LCG.

Lithium grease, as the most commonly used lubricating grease, has been extensively studied regarding the influence of nano-additives on its wear-resistant and anti-friction properties. For example, Kumar, N et al. found that adding 2 wt% of Talc nanoparticles to lithium grease can improve its wear resistant capability by 45%, and also reduces its friction coefficient [1]. He, Q et al. found that after adding 0.6 wt% of nanometer-CeO<sub>2</sub> to lithium grease, the friction coefficient and wear scar diameter decreased by 28% and 13% compared with base grease, respectively [3]. However, Wu, C et al. found that adding 0.6 wt% of nanometer-CuO to lithium grease causes fluctuations in the COF and reduces the anti-wear performance of the lithium-based grease, with the wear diameter increasing by 21.7% compared to the original grease [4]. They also tested the frictional properties of lithium grease with the addition of 1 wt% of carbon black, Fe<sub>3</sub>O<sub>4</sub>, and Al<sub>2</sub>O<sub>3</sub> nanoparticles. The wear volume decreased by 6.5%, 17%, and 19.9%, respectively. Similar to FLG, Al<sub>2</sub>O<sub>3</sub> nanoparticles can improve the anti-wear performance of the grease by depositing on the friction pair surface. Additionally, Al<sub>2</sub>O<sub>3</sub> can promote the flow of the base oil to reduce the vibration of the friction pair [5].

By comparing the effects of the above-mentioned nano-additives on the frictional properties of lithium grease, it is easy to find that although 1 wt% FLG can enhance the wear-resistant and anti-friction performance of LCG, it still has certain shortcomings compared to nano-additives such as Talc nanoparticles and Al<sub>2</sub>O<sub>3</sub>. For instance, 2 wt% Talc nanoparticles can simultaneously improve the wear-resistant and anti-friction properties of lithium grease, while 1 wt% FLG can only enhance either the wear-resistant or anti-friction performance of LCG, and the degree of improvement is weaker than that achieved by 2 wt% Talc nanoparticles. Adding 1 wt% of Al<sub>2</sub>O<sub>3</sub> to LCG can reduce the vibration of the

friction pair. However, as shown in Figures 5a, 6a, 7a and 8a, the fluctuation degree of the friction curves of LCG with different FLG contents did not significantly decrease. This indicates that FLG lacks the ability to reduce the vibration of the friction pair under the four test conditions.

Research on the influence of FLG on the frictional properties of LCG is limited. Only Li et al. tested the effect of FLG on the frictional properties of lithium grease. FLG contents in lithium greases were 0.05 wt%, 0.1 wt%, and 0.2 wt%, tested by the four-ball tribotester (MR-10P). The test covered speeds ranging from 600 to 1450 r/min, with loads of 294 N, 392 N, 490 N, 588 N, and 686 N, at ambient temperature. The experimental results demonstrate that 0.1%wt of FLG can enhance the wear-resistant and anti-friction performance of lithium grease under high speeds and high loads [27]. The FLG content added to the LCG in this study was 0.5 wt%, 1 wt%, and 2 wt%, with loads of 10 N and 100 N and testing temperatures of 30 °C and 100 °C. The novelty lies in the FLG content, testing loads, and testing temperatures, which demonstrate a higher level of innovation.

### 3.3. Frictional Mechanism Analysis

To further understand the composition of the friction product and the effect of FLG and temperature on the friction product, XPS analysis was performed on the surface of steel plates lubricated with pure LCG and LCG + 1 wt% FLG under high load conditions.

Figures 9–12 show the results of XPS analysis of C1s, O1s, Fe2p, and Li1s on the worn surface of the steel plate, respectively. From Figure 9, it can be seen that the C-C bond (284.7 eV), C-OLi bond (285.8 eV), C-O bond (288.3 eV), and C=O bond (292.6 eV) existed on the worn surface, indicating that the thickener molecules in the LCG were chemisorbed with the metal surface and formed a chemisorbed film.

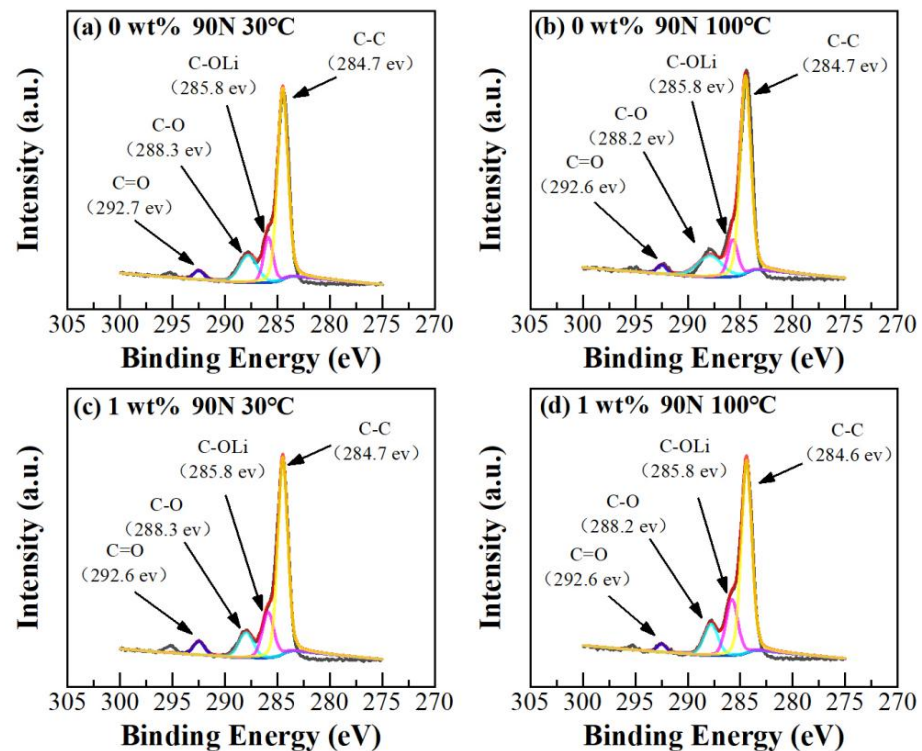


Figure 9. XPS analysis results of C1s on the worn surface of steel plates.

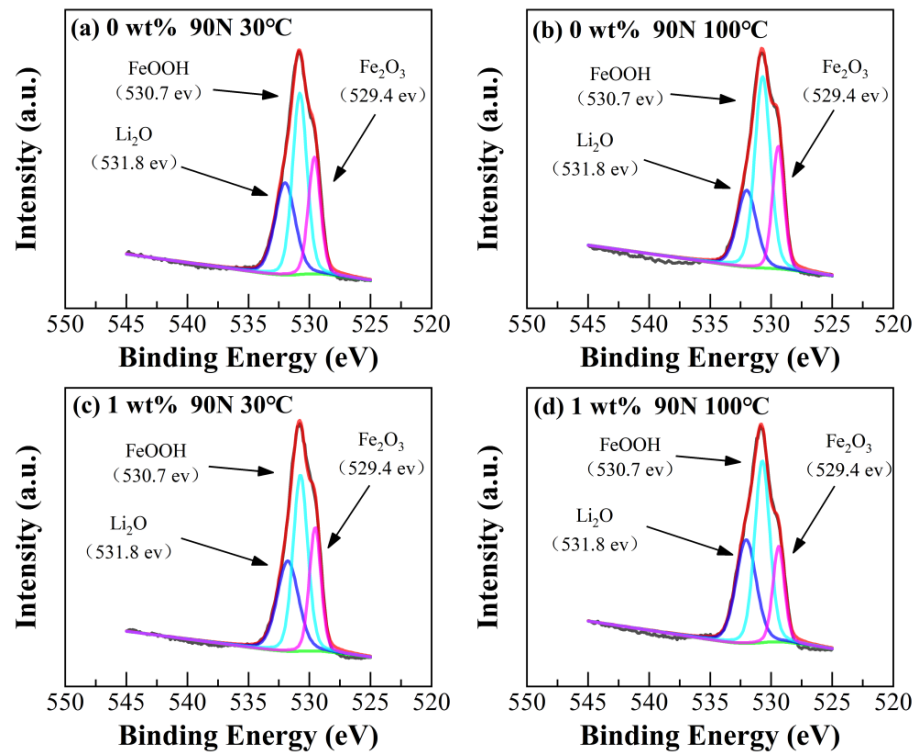


Figure 10. XPS analysis results of O1s on the worn surfaces of steel plates.

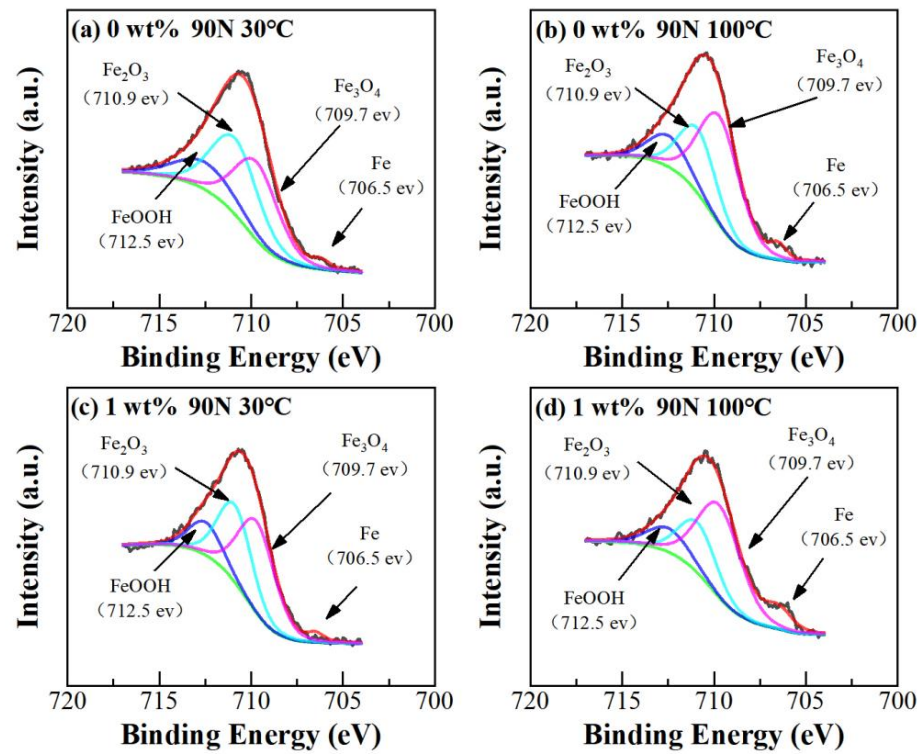


Figure 11. XPS analysis results of Fe2p on the worn surfaces of steel plates.

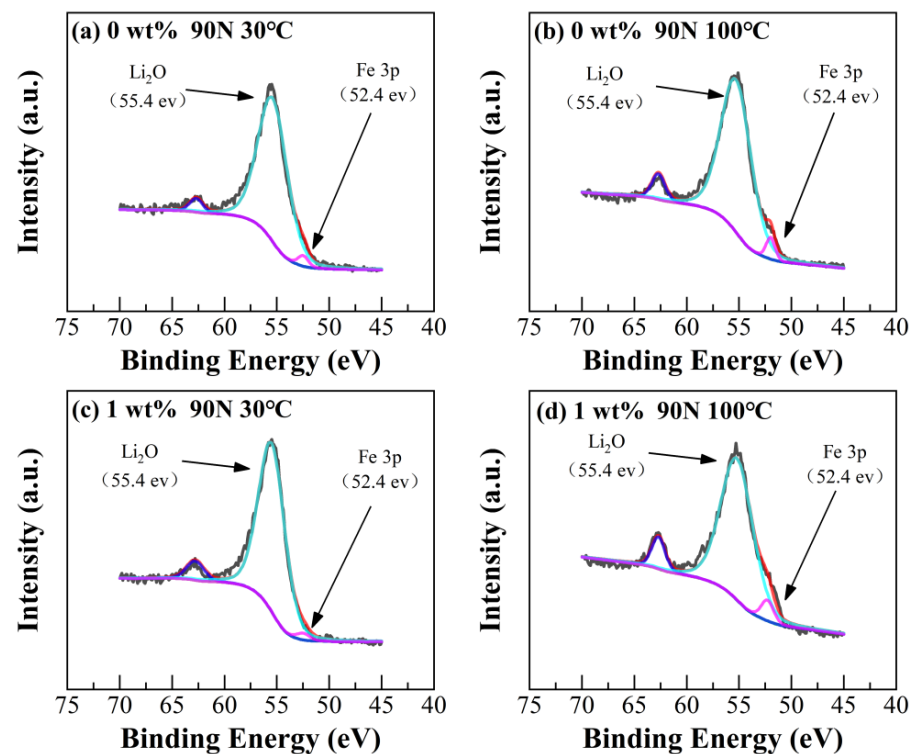
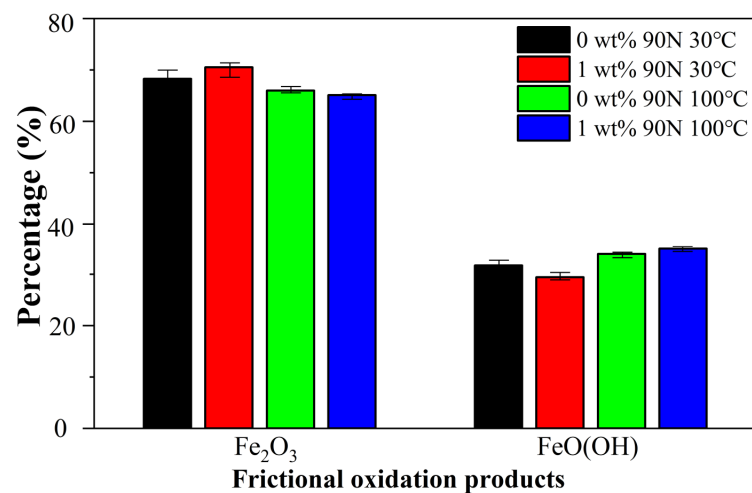


Figure 12. XPS analysis results of Li1s on the worn surfaces of steel plates.

In Figures 10 and 11, the O1s peak at 531.0 eV and the Fe2p peak near 710.9 eV are characteristics of  $\text{Fe}_2\text{O}_3$ , and the O1s peak at 529.8 eV and the Fe2p peak near 712.5 eV are characteristics of  $\text{FeO}(\text{OH})$  [8,35]. This proves that  $\text{Fe}_3\text{O}_4$ ,  $\text{Fe}_2\text{O}_3$ , and  $\text{FeO}(\text{OH})$  are also formed on the friction surface after LCG lubrication. Similarly,  $\text{Fe}_3\text{O}_4$  is formed by the natural oxidation of GCr15-bearing steel in the air, and  $\text{Fe}_2\text{O}_3$  and  $\text{FeO}(\text{OH})$  are formed under high-friction heat. The large amount of friction heat during the friction process can promote friction oxidation, which increases the production of the friction products  $\text{FeO}(\text{OH})$  and  $\text{Fe}_2\text{O}_3$  while facilitating the conversion of amorphous  $\text{FeO}(\text{OH})$  to crystalline  $\text{Fe}_2\text{O}_3$ . Since the effect of  $\text{FeO}(\text{OH})$  and  $\text{Fe}_2\text{O}_3$  in the friction does not alter due to the change of grease type, the non-crystalline  $\text{FeO}(\text{OH})$  still plays a role in improving the toughness of the oxide film and reducing the role of interfacial friction. At the same time, the crystalline  $\text{Fe}_2\text{O}_3$  is easy to peel off and fall off as abrasive chips in the oxidative wear process. Frictional oxidation products are continuously generated and also continuously consumed by wear in the friction process, which is a dynamic process.

In Figures 10 and 12, the O1s peak at 531.8 eV and the Li1s peak at 55.4 eV are characteristic of  $\text{Li}_2\text{O}$  [36], indicating that during the friction process, lithium dodecahydroxystearate, and lithium sebacate in the LCG thickener are oxidized to form a  $\text{Li}_2\text{O}$  friction film due to locally elevated temperature, revealing the lubricating effect of the grease thickener. The lubricating film formed by the thickener works with the oxidizing film composed of  $\text{Fe}_2\text{O}_3$ ,  $\text{FeO}(\text{OH})$ , and  $\text{Li}_2\text{O}$  to play a critical protective role against frictional forces.

Figure 13 shows the ratios of  $\text{Fe}_2\text{O}_3$  and  $\text{FeO}(\text{OH})$  in the friction oxidation product. Under high load and high-temperature conditions, the steel plate lubricated with the LCG + 1 wt% FLG has the highest percentage of  $\text{FeO}(\text{OH})$  and minimal SPAV; in contrast, under elevated load and low-temperature conditions, the steel plate lubricated with the LCG + 1 wt% FLG has the smallest percentage of  $\text{FeO}(\text{OH})$  and the highest SPAV. This phenomenon indicates that the proportion of  $\text{FeO}(\text{OH})$  in the frictional oxidized product is related to its wear. The larger the proportion of  $\text{FeO}(\text{OH})$  in the frictional oxidized product, the smaller the abrasion volume of its corresponding steel plate.



**Figure 13.** Proportion of Fe<sub>2</sub>O<sub>3</sub> and FeO(OH) in friction oxidation products.

A large amount of friction heat in the friction process will promote friction oxidation, increase the friction products FeO(OH) and Fe<sub>2</sub>O<sub>3</sub>, and promote the conversion of amorphous FeO(OH) to crystalline Fe<sub>2</sub>O<sub>3</sub>. The dynamic equilibrium reached at different ambient temperatures is different. Under the action of LCG, the proportion of FeO(OH) increases under high-temperature conditions, indicating that the ambient temperature has little influence on it, and the friction heat generated by friction is the main influencing factor.

Under high load and low-temperature conditions, the anti-friction and wear-resistant effect of LCG + 1 wt% FLG is not ideal, and the friction process will generate a lot of friction heat, an increase in temperature not only accelerates oxidation reactions but also facilitates the transformation of amorphous FeO(OH) into crystalline Fe<sub>2</sub>O<sub>3</sub> [37]. An increase in temperature not only accelerates oxidation reactions but also facilitates the transformation of amorphous FeO(OH) into crystalline Fe<sub>2</sub>O<sub>3</sub> [37]. Thus, the proportion of FeO(OH) is lower than that of pure LCG. Under high load and high-temperature conditions, LCG + 1 wt% FLG has obvious anti-friction effects, reducing the friction heat generated during the friction process, and the thermal conductivity of FLG also reduces friction heat [11], which jointly inhibits the conversion of amorphous FeO(OH) to crystalline Fe<sub>2</sub>O<sub>3</sub>, so the proportion of FeO(OH) is higher than that of pure LCG.

### 3.4. The Establishment of Frictional Mechanism Models

Based on the above analysis, the frictional mechanism models of pure LCG and LCG containing FLG were obtained. The frictional mechanism model is shown in Figure 14. Under the action of pure LCG, the lubrication film on the plate surface comprised of chemical adsorption film formed by the thickener molecule adsorbed on the metal surface and tribochemical reaction film consists of FeO(OH), Fe<sub>2</sub>O<sub>3</sub>, Fe<sub>3</sub>O<sub>4</sub>, Li<sub>2</sub>O, and other oxides (Figure 14a). Serving as the chief element of lubricating film, the chemisorbed film of thickener has the bearing capacity to prevent direct contact between friction pairs. Under the action of LCG containing FLG, the tribochemical reaction film comprised of oxides occupies a crucial position in minimizing friction and wear. The thickener chemisorbed film, the FLG deposition film, and the friction reaction film combine into a boundary-lubricating film on the friction surface (Figure 14b). FLG has a nanoscale morphology and is easily filled into the depression of the friction pair [14,38]; its deposition film can repair worn surfaces and avoid direct metal-to-metal contact during lubrication, providing superior lubrication while minimizing abrasion and friction.

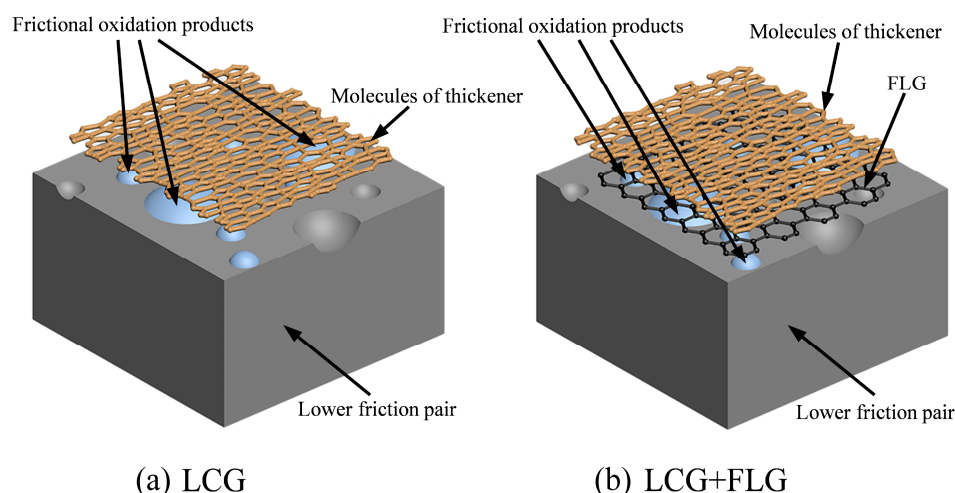


**Figure 14.** Schematic drawing of frictional mechanism model: (a) LCG; (b) LCG + FLG.

Figure 15 shows the enlarged perspective of the abrasion scar lubricated with LCG and LCG + 1 wt% FLG under 90 N and 100 °C taken with a MIT300 metallurgical microscope. To validate the proposed mechanism model, a comparison was made between the abrasion scars observed under lubrication with pure LCG and observed with LCG + 1 wt% FLG. As depicted in Figure 15a, the abrasion scar lubricated with pure LCG exhibited denser furrows than that of LCG + 1 wt% FLG. The existence of a large amount of brittle exfoliation on the worn surface also indicates that serious adhesive wear occurs. Conversely, Figure 15b reveals that the furrows on the plate surfaces lubricated with LCG + 1 wt% FLG are finer and less dense, with reduced brittle exfoliation. This suggests that the FLG deposition film effectively shields the friction surface and replenishes and repairs abrasion scars, thereby minimizing direct contact between the friction pair. FLG has excellent thermal conductivity, which can also reduce the friction heat in the friction process and prevent the conversion of amorphous FeO(OH) into Fe<sub>2</sub>O<sub>3</sub> crystallization, consequently decreasing oxidative wear.

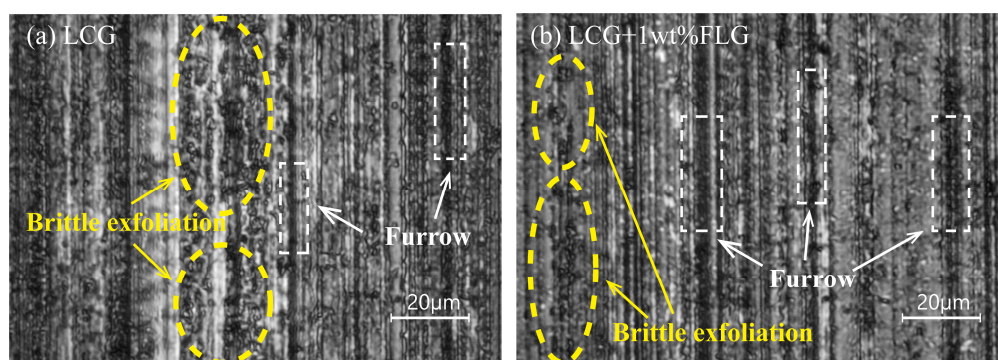


**Figure 15.** The enlarged perspective of the abrasion scar lubricated with LCG and LCG + 1 wt% FLG under 90 N and 100 °C.

#### 4. Conclusions

The effects of FLG content on the frictional properties of LCG under different temperatures and working conditions were studied by the SRV-5 rubbing and abrasion tester. According to the influence of few-layer graphene (FLG) on the friction characteristics of lithium compound grease (LCG), the following conclusions are finally drawn:

1. Under low load and low-temperature conditions, the fiber structure of pure LCG has a strong deformation resistance and the resulting lubricating film is more stable and can protect the friction surface. At this time, there is no abrasive wear on the surface of the steel plate, and the wear type is oxidative wear and minor abrasive wear. However,

the fluidity of LCG at low temperatures is poor, and FLG is not easily dispersed in LCG, which reduces the anti-friction performance of LCG. The more FLG content in LCG, the easier it is to gather during friction. FLG cannot reduce the energy barrier in the aggregation state but plays the role of wear particles in the friction process, causing abrasive wear, increasing the furrow of the friction surface, and thus reducing the wear-resistant performance of LCG.

2. Under the condition of low load and high temperature, FLG has no obvious improvement in the anti-friction performance of LCG. The abrasion scars of the four greases are shallow and the wear type is oxidative wear, which indicates that LCG can protect the friction surface well under low load and high-temperature conditions. However, only a moderate amount of FLG (1 wt%) can improve the wear-resistant performance of LCG, too little or excessive FLG will increase wear loss.
3. Under the condition of high load and low temperature, FLG in LCG is easy to aggregate, which hinders lubrication and causes the stress concentration in the middle of the steel plate, forming deeper gullies, and the wear type is mainly abrasive wear. The poor fluidity of LCG at low temperatures contributes to inadequate dispersion of FLG, facilitating aggregation and reducing the anti-friction performance of LCG. The COF and SPAV of the four lithium compound greases are significantly higher compared to those under the other three conditions, indicating that the LCG used in this test is not suitable for high-load and low-temperature applications.
4. Under the condition of high load and high temperature, the steel plate lubricated with LCG + 1 wt% FLG exhibits lower COF and SPAV, but the difference in SPAV can also be considered even within the error scattering range, and the wear type of the steel plate under its lubrication is oxidative wear and abrasive wear. An appropriate amount of FLG (1 wt%) can slightly improve the anti-friction properties of LCG but has no obvious improvement on wear-resistant performance.
5. The frictional mechanism model of LCG adding FLG was derived based on the friction test results, XPS analysis results, and the enlarged wear morphology of the steel plate surface. The thickener chemisorbed film, the FLG deposition film, and the friction reaction film combine into a boundary lubricating film on the friction surface. Its deposition film can repair the worn surfaces and avoid direct metal-to-metal contact during lubrication, providing superior lubrication while minimizing abrasion and friction.

Within the operating range of 1 GPa to 2.06 GPa and 30 °C to 100 °C under only elevated temperature and low load conditions, adding 1 wt% FLG to LCG can only improve its wear-resistant property. Under elevated temperatures and high load conditions, adding 1 wt% FLG to LCG can only enhance the anti-friction characteristics of LCG. Conversely, under all low temperature conditions, the incorporation of FLG into LCG has a negative effect.

**Author Contributions:** Conceptualization, Y.W. and Z.L.; data curation, Z.L.; investigation, X.G.; methodology, Y.W.; project administration, Y.W.; validation, M.W.; visualization, Z.L. and Q.Q.; writing—original draft, Y.W., Z.L. and X.G.; writing—review and editing, Y.W. and Z.L. visualization, Z.L.; supervision, Y.W.; project administration, Y.W.; funding acquisition, Y.W. All authors have read and agreed to the published version of the manuscript.

**Funding:** This research was funded by National Natural Science Foundation of China (Grant No. 52075274) and Shandong Provincial Key Research and Development Program (Major Science and Technology Innovation Project) (Grant No. 2022CXGC010304).

**Institutional Review Board Statement:** Not applicable.

**Informed Consent Statement:** Not applicable.

**Data Availability Statement:** Data are contained within the article.

**Conflicts of Interest:** The authors declare no conflicts of interest.

### Abbreviations

FLG	few-layer graphene
COF	friction coefficient
LCG	lithium compound grease
SPAV	abrasion volume of steel plate

### References

- Kumar, N.; Vinay, S.; Jayashree, B. Exploration of Talc nanoparticles to enhance the performance of Lithium grease. *Tribol. Int.* **2021**, *162*, 107107. [[CrossRef](#)]
- Kumar, N.; Saini, V.; Bijwe, J. Performance properties of lithium greases with PTFE particles as additive: Controlling parameter-size or shape? *Tribol. Int.* **2020**, *148*, 106302. [[CrossRef](#)]
- He, Q.; Li, A.; Guo, Y.; Liu, S.-F.; Zhang, Y.; Kong, L.-H. Tribological properties of nanometer cerium oxide as additives in lithium grease. *J. Rare Earths* **2018**, *36*, 209–214. [[CrossRef](#)]
- Wu, C.; Xiong, R.-F.; Ni, J.; Yao, L.; Chen, L.; Li, X.-L. Effects of CuO nanoparticles on friction and vibration behaviors of grease on rolling bearing. *Tribol. Int.* **2020**, *152*, 106552. [[CrossRef](#)]
- Wu, C.; Kai, Y.; Ying, C.; Ni, J.; Yao, L.; Li, X.-L. Investigation of friction and vibration performance of lithium complex grease containing nano-particles on rolling bearing. *Tribol. Int.* **2020**, *155*, 106761. [[CrossRef](#)]
- Wu, C.; Hong, Y.-Y.; Ni, J.; Teal, P.-D.; Yao, L.; Li, X.-L. Investigation of mixed hBN/Al<sub>2</sub>O<sub>3</sub> nanoparticles as additives on grease performance in rolling bearing under limited lubricant supply. *Colloid Surf. A Physicochem. Eng. Asp.* **2023**, *659*, 130811. [[CrossRef](#)]
- Wu, C.; Li, S.-S.; Chen, Y.; Yao, L.; Li, X.-L.; Ni, J. Tribological properties of chemical composite and physical mixture of ZnO and SiO<sub>2</sub> nanoparticles as grease additives. *Appl. Surf. Sci.* **2023**, *612*, 155932. [[CrossRef](#)]
- Zhu, L.-L.; Wu, X.-H.; Zhao, G.-Q.; Wang, X.-B. Tribological characteristics of bisphenol AF bis(diphenyl phosphate) as an antiwear additive in polyalkylene glycol and polyurea grease for significantly improved lubrication. *Appl. Surf. Sci.* **2016**, *363*, 145–153. [[CrossRef](#)]
- Berman, D.; Erdemir, A.; Sumant, V.A. Graphene: A new emerging lubricant. *Mater. Today* **2014**, *17*, 31–42. [[CrossRef](#)]
- Niu, M.; Qu, J.-J.; Gu, L. Synthesis of titanium complex grease and effects of graphene on its tribological properties. *Tribol. Int.* **2019**, *140*, 105815. [[CrossRef](#)]
- Min, X.; Jun, C.; Huo, C.-X.; Zhao, G.-H. Improving the lubricity of a bio-lubricating grease with the multilayer graphene additive. *Tribol. Int.* **2020**, *150*, 106386. [[CrossRef](#)]
- Yu, W.; Xie, H.-Q.; Chen, L.-F.; Zhu, Z.-G.; Zhao, J.-C.; Zhang, Z.-H. Graphene based silicone thermal greases. *Phys. Lett. A* **2014**, *378*, 207–211. [[CrossRef](#)]
- Mao, J.-Y.; Chen, G.-Y.; Zhao, J.; He, Y.-Y.; Luo, J.-B. An investigation on the tribological behaviors of steel/copper and steel/steel friction pairs via lubrication with a graphene additive. *Friction*. **2020**, *9*, 228–238. [[CrossRef](#)]
- Zhao, J.; Mao, J.; Li, Y.; He, Y.; Luo, J. Friction-induced nano-structural evolution of graphene as a lubrication additive. *Appl. Surf. Sci.* **2018**, *434*, 21–27. [[CrossRef](#)]
- Wang, X.-B.; Zhang, Y.-F.; Yin, Z.-W.; Su, Y.-J.; Zhang, Y.-P.; Cao, J. Experimental research on tribological properties of liquid phase exfoliated graphene as an additive in SAE 10W-30 lubricating oil. *Tribol. Int.* **2019**, *135*, 29–37. [[CrossRef](#)]
- Zheng, D.; Cai, Z.-B.; Shen, M.-X.; Li, Z.-Y.; Zhu, M.-H. Investigation of the tribology behaviour of the graphene nanosheets as oil additives on textured alloy cast iron surface. *Appl. Surf. Sci.* **2016**, *387*, 66–75. [[CrossRef](#)]
- Wang, J.; Guo, X.-C.; He, Y.; Jiang, M.-J.; Gu, K.-C. Tribological characteristics of graphene as grease additive under different contact forms. *Tribol. Int.* **2018**, *127*, 457–469. [[CrossRef](#)]
- Cheng, Z.-L.; Qin, X.-X. Study on friction performance of graphene-based semi-solid grease. *Chin. Chem. Lett.* **2014**, *25*, 1305–1307. [[CrossRef](#)]
- Zhang, J.; Wang, A.; Yin, H.-B. Preparation of graphite nanosheets in different solvents by sand milling and their enhancement on tribological properties of lithium-based grease. *Chin. J. Chem. Eng.* **2020**, *28*, 1177–1186. [[CrossRef](#)]
- Deng, X.; Huang, J.; Liu, C.-H.; Gan, L.; Hong, J.; Liu, W.-F.; Luo, L.-H.; Wang, Y. Coupling hybrid of graphene oxide and layered zirconium phosphonate to enhance phenolic resin-based friction materials. *J. Appl. Polym. Sci.* **2018**, *135*, 46543. [[CrossRef](#)]
- Zulhanafi, P.; Syahrullail, S.; Faizin, Z.-N. Tribological performance of trimethylolpropane ester bio-lubricant enhanced by graphene oxide nanoparticles and oleic acid as a surfactant. *Tribol. Int.* **2023**, *183*, 108398. [[CrossRef](#)]
- Ouyang, T.-C.; Shen, Y.-D.; Yang, R.; Liang, L.-Z.; Liang, H.; Lin, B.; Tian, Z.-Q.; Shen, P.-K. 3D hierarchical porous graphene nanosheets as an efficient grease additive to reduce wear and friction under heavy-load conditions. *Tribol. Int.* **2020**, *144*, 106118. [[CrossRef](#)]
- Zhai, H.-B.; Jia, L.-H.; Yang, W.-B.; Wu, P.; Jian, H.; Liu, C.-J.; Jiang, W. Effect of g-C<sub>3</sub>N<sub>4</sub> morphology on its performance as lubricating additive for grease. *J. Appl. Polym. Sci.* **2023**, *660*, 130831. [[CrossRef](#)]
- Bai, T.; Geng, F. Investigate on the tribological properties of additives in tetra polyurea grease. In Proceedings of the 2018 First International Conference on Environment Prevention and Pollution Control Technology (EPPCT 2018), Tokyo, Japan, 9–11 November 2018; School of Material Science and Engineering, Shanghai Institute of Technology: Shanghai, China; Suzhou Huifeng Lubricant Co., Ltd.: Suzhou, China; Department of Chemistry and Materials Engineering, Changshu Institute of Technology: Changshu, China, 2018. [[CrossRef](#)]

25. Jin, B.; Zhao, J.; Chen, G.-Y.; He, Y.-Y.; Huang, Y.-Y.; Luo, J.-B. In situ synthesis of  $Mn_3O_4$ /graphene nanocomposite and its application as a lubrication additive at high temperatures. *Appl. Surf. Sci.* **2021**, *546*, 149019. [[CrossRef](#)]
26. Wu, J.; Mu, L.-W.; Zhu, J.-H.; Feng, X.; Lu, X.-H.; Larsson, R.; Shi, Y.-J. Synthesis of hollow fullerene-like molybdenum disulfide/reduced graphene oxide nanocomposites with excellent lubricating properties. *Carbon* **2018**, *134*, 423–430. [[CrossRef](#)]
27. Li, Z.-J.; He, Q.; Du, S.-M.; Zhang, Y.-Z. Effect of few layer graphene additive on the tribological properties of lithium grease. *Lubr. Sci.* **2020**, *32*, 333–343. [[CrossRef](#)]
28. Cheng, Z.-L.; Kong, Y.-C.; Fan, L.; Liu, Z. Ultrasound-assisted  $Li^+/Na^+$  co-intercalated exfoliation of graphite into few-layer graphene. *Ultrason. Sonochem.* **2020**, *66*, 105–108. [[CrossRef](#)]
29. Sun, Z.; Xu, C.-M.; Peng, Y.-X.; Shi, Y.-Y.; Zhang, Y.-W. Fretting tribological behaviors of steel wires under lubricating grease with compound additives of graphene and graphite. *Wear* **2020**, *454*, 202333. [[CrossRef](#)]
30. Mohamed, A.; Tirth, V.; Kamel, M.-B. Tribological characterization and rheology of hybrid calcium grease with graphene nanosheets and multi-walled carbon nanotubes as additives. *J. Mater. Res. Technol.* **2020**, *9*, 6178–6185. [[CrossRef](#)]
31. GB/T308-2002; Rolling Bearings—Steel Balls. Standardization Administration of the People’s Republic of China: Beijing, China, 2003.
32. Hamrock, B.J.; Dowson, D. Isothermal Elastohydrodynamic Lubrication of Point contacts: Part VI—Starvation Results. *J. Lubr. Technol.* **1977**, *99*, 15–23. [[CrossRef](#)]
33. Parashar, A.; Mertiny, P. Effect of van der Waals Forces on the Buckling Strength of Graphene. *J. Comput. Theor. Nanosci.* **2013**, *10*, 2626–2630. [[CrossRef](#)]
34. Huang, J.; Zhao, X.; Ma, C.; Cheng, Y.; Zhang, J. Preparation of Few-Layer Porous Graphene by a Soft Mechanical Method with a Short Rolling Transfer Process. *ChemPlusChem* **2020**, *85*, 2482–2486. [[CrossRef](#)]
35. Xiong, S.; Zhang, B.-S.; Luo, S.; Wu, H.; Zhang, Z. Preparation, characterization, and tribological properties of silica-nanoparticle-reinforced B-N-co-doped reduced graphene oxide as a multifunctional additive for enhanced lubrication. *Friction* **2020**, *9*, 239–249. [[CrossRef](#)]
36. Zhao, J.; Li, Y.-R.; Mao, J.-Y.; He, Y.-Y.; Luo, J.-B. Synthesis of thermally reduced graphite oxide in sulfuric acid and its application as an efficient lubrication additive. *Tribol. Int.* **2017**, *116*, 303–309. [[CrossRef](#)]
37. Zhang, C.X.; Song, Z.Q.; Liu, Z.F.; Cheng, Q.; Zhao, Y.S.; Yang, C.B.; Liu, M.M. Wear mechanism of fexspline materials regulated by novel amorphous/crystalline oxide form evolution at frictional interface. *Tribol. Int.* **2019**, *135*, 335–343. [[CrossRef](#)]
38. Chouhan, A.; Mungse, H.P.; Sharma, O.P.; Singh, R.K.; Khatri, O.P. Chemically functionalized graphene for lubricant applications: Microscopic and spectroscopic studies of contact interfaces to probe the role of graphene for enhanced tribo-performance. *Colloid Interface Sci.* **2018**, *513*, 666–676. [[CrossRef](#)]

**Disclaimer/Publisher’s Note:** The statements, opinions and data contained in all publications are solely those of the individual author(s) and contributor(s) and not of MDPI and/or the editor(s). MDPI and/or the editor(s) disclaim responsibility for any injury to people or property resulting from any ideas, methods, instructions or products referred to in the content.